current issues in molecular biology

MDPI

Article

Transcriptomic Analysis of Flower Development Under Hot Ambient Temperatures and Identification of Genes Associated with Heat Tolerance in Passion Fruit

Yanyan Wu [1,†], Jieyun Liu [1,†], Qinglan Tian [1], Weihua Huang [1], Junniu Zhou [1], Xinghai Yang [2,*] and Haifei Mou [1,*]

[1] Biotechnology Research Institute, Guangxi Academy of Agricultural Sciences, Nanning 530007, China; wuyanyan@gxaas.net (Y.W.); jieyunliu@gxaas.net (J.L.); tianqinglan@gxaas.net (Q.T.); huangweihua@gxaas.net (W.H.); 1121.zjn@gxaas.net (J.Z.)

[2] Guangxi Key Laboratory of Rice Genetics and Breeding, Rice Research Institute, Guangxi Academy of Agricultural Sciences, Nanning 530007, China

* Correspondence: yangxinghai888@gxaas.net or yangxinghai514@163.com (X.Y.); mhf@gxaas.net (H.M.)

† These authors contributed equally to this work.

Abstract

Elevated ambient temperatures (32 °C) severely inhibit floral bud initiation and floral organ development in passion fruit. Although the cultivar Jinlingziguo exhibits relatively high heat tolerance and can flower and set fruit under high-temperature conditions, the molecular mechanisms underlying floral development during heat stress remain unclear. Here, we performed transcriptome sequencing at three stages of floral bud development in two passion fruit germplasms with contrasting heat tolerance, Jinlingziguo and Huangguoyuanshengzhong, to characterize their transcriptional responses to high temperature. Sequencing of 18 samples generated 129.58 Gb of clean data and identified 32,373 expressed genes and 56,265 transcripts. Across the three developmental stages, we identified 7529 differentially expressed genes (DEGs), with downregulated genes outnumbering upregulated genes at each stage. KEGG pathway enrichment analysis highlighted stress-response pathways, mitogen-activated protein kinase (MAPK) signaling, plant hormone signal transduction, and starch and sucrose metabolism. Weighted gene co-expression network analysis (WGCNA) identified the pink and green-yellow modules as key co-expression modules. The pink module was enriched in MAPK signaling and plant hormone signal transduction, whereas the green-yellow module was enriched in pathways involving basal transcription factors and plant hormone signal transduction. *ZX.04G0014930* and *ZX.01G0041270* were identified as hub genes in the pink and green-yellow modules, respectively. We also identified 28 heat shock factor (HSF) family members and predicted 2537 potential target genes. Gene Ontology (GO) enrichment analysis associated eight of these targets with responses to temperature stimuli and 13 with responses to abiotic stimuli. KEGG analysis linked three predicted targets to the plant MAPK signaling pathway and four to plant hormone signal transduction. Further studies indicated that the homologous genes of *ZX.01G0041270* in *Arabidopsis* and rice are involved in the regulation of ABA signal transduction, suggesting that *ZX.01G0041270* may play an important role in the adaptation of passion fruit to high-temperature environments. This study constructed a transcriptional regulatory network of passion fruit in response to high temperature, revealed the roles of MAPK signaling and hormone signaling in regulation, and analyzed the potential functions of the HSF family and their target genes in high-temperature response, providing gene resources and a theoretical basis for thermotolerance breeding.

Check for updates

Academic Editors: Tuo Ji and Fengjuan Yang

Received: 26 October 2026
Revised: 16 November 2026
Accepted: 19 November 2026
Published: 20 November 2026

Copyright: © 2026 by the authors. Licensee MDPI, Basel, Switzerland. This article is an open access article distributed under the terms and conditions of the Creative Commons Attribution (CC BY) license.

Keywords: passion fruit; hot ambient temperatures; RNA sequencing (RNA-seq); heat tolerance; candidate gene; abscisic acid (ABA)

1. Introduction

Passion fruit (*Passiflora edulis*) is a tropical and subtropical fruit crop characterized by high nutritional value and a distinctive aroma [1]. Its economic value and suitability for processing have supported cultivation worldwide. However, passion fruit is sensitive to elevated temperatures, and increasingly hot summers associated with global warming pose a major challenge to production. Heat stress can impair photosynthesis and plant growth, shorten the flowering period, disrupt floral bud differentiation, reduce fruit set, and cause fruit malformation and abscission [2], leading to substantial yield losses. Understanding the molecular mechanisms of heat-stress responses and identifying genetic resources associated with heat tolerance are therefore important for developing resilient cultivars and supporting sustainable passion fruit production.

Plant responses to high-temperature stress involve complex biological processes that require the coordinated regulation of multiple physiological and metabolic pathways, including photosynthetic regulation, activation of antioxidant defense systems, maintenance of osmotic homeostasis, and hormone signal transduction [3,4]. Advances in high-throughput sequencing and bioinformatics, together with the availability of a high-quality passion fruit reference genome, have enabled more systematic investigations of heat tolerance in this species. Numerous studies have characterized the basic features of the heat-stress response in passion fruit at the physiological, biochemical, metabolomic, and transcriptomic levels. These include heat-induced accumulation of malondialdehyde, reductions in the photochemical efficiency of photosystem II [4], and dynamic changes in antioxidant enzyme activities. Exogenous compounds such as glycine betaine can mitigate heat damage by affecting carbon and nitrogen metabolism, while endogenous hormones, including cytokinins, can partially counteract gibberellin-induced floral organ abortion. These findings suggest that hormonal crosstalk plays a critical role in the heat adaptation of passion fruit flowers [3].

Transcription factors are central regulators of plant responses to environmental stress. Several transcription factor families implicated in heat responses have been identified in passion fruit, including heat shock factors (HSFs), Dof, TCP, TALE, BAG, and bZIP proteins. Among these, HSFs are key regulators of heat-stress signaling. A total of 15–18 PeHSF members have been identified in passion fruit and exhibit differential expression in response to high temperature and other treatments. Moreover, heterologous overexpression of *PeHSF-C1a* significantly enhances heat tolerance in *Arabidopsis thaliana*, likely through the upregulation of downstream heat shock proteins and stress-responsive genes [5,6]. In addition, the Dof family member *PeDof-11* [7] and the BAG family genes *PeBAG4-3* and *PeBAG6-1* have been shown to be strongly induced under high-temperature conditions [8], suggesting that these transcription factors collectively form a complex regulatory network governing the heat-stress response in passion fruit. Furthermore, some members of the TALE [9] and bZIP [10] families not only respond to heat stress but also participate in the regulation of floral organ development, providing new molecular clues for understanding heat-induced floral abortion.

Despite these advances, important questions remain about the molecular basis of heat tolerance in passion fruit. In particular, the cooperative and antagonistic relationships among transcription factor families are not well understood, nor is it clear how heat-stress signaling is integrated with hormone signaling and developmental programs to determine

floral organ fate. Few studies have systematically examined the mechanisms that allow heat-tolerant germplasm to maintain normal floral development under elevated temperatures. To address this gap, we compared the transcriptomes of two germplasms with contrasting heat tolerance—Jinlingziguo (heat-tolerant) and Huangguoyuanshengzhong (heat-sensitive)—at three key stages of floral bud development. We aimed to characterize the molecular responses associated with floral development under heat stress and identify candidate signaling pathways and hub genes related to heat tolerance. These findings may inform the molecular breeding of heat-tolerant passion fruit cultivars.

2. Materials and Methods

2.1. Plant Materials

The heat-tolerant passion fruit cultivar Jinlingziguo and the heat-sensitive germplasm Huangguoyuanshengzhong were grown at the Meili Nanfang Experimental Station in Nanning, Guangxi, China. For the high-temperature treatment, a steel-pipe frame (10.0 m long × 2.0 m wide × 4.0 m high) was installed over the planting rows. The frame was covered with transparent plastic film (light transmittance > 95%) to raise the internal temperature, while 20 cm-high openings along the upper edges of both sides permitted air exchange. Before treatment, the structure remained fully open so that experimental and control plants experienced the same natural conditions. Heat treatment began when secondary vines emerged. The film was then lowered over the top and sides of the structure, and the internal temperature was monitored continuously. Under heat treatment, the maximum daytime temperature was maintained at 38–45 °C, the daily mean temperature at 30–31 °C, and the temperature remained ≥35 °C for 4–6 h per day, with relative humidity inside the structure maintained above 30%. Under natural control conditions, the maximum daytime temperature was <37 °C, the daily mean temperature was <28.5 °C, and the temperature remained ≥35 °C for <2 h per day. The treatments were maintained continuously for 40 days. Samples were collected on days 16, 24, and 32 of floral bud differentiation.

2.2. mRNA Extraction and cDNA Library Construction

Total RNA was extracted from tissue samples, and its concentration and purity were determined using a micro-volume UV-Vis spectrophotometer NanoDrop 2000 (Thermo Fisher Scientific, Waltham, MA, USA). RNA integrity was assessed by agarose gel electrophoresis, and RNA quality numbers (RQNs) were determined using an Agilent 5300 Fragment Analyzer (Agilent Technologies, Santa Clara, CA, USA). RNA samples used for library construction were required to have a total RNA amount of at least 1 μg, a concentration of ≥30 ng/μL, an RQN > 6.5, and an OD260/280 ratio of 1.8–2.2. Polyadenylated mRNA was enriched using oligo(dT)-coupled magnetic beads and fragmented to approximately 300 bp in fragmentation buffer. First-strand cDNA was synthesized from the fragmented RNA using reverse transcriptase and random primers, followed by second-strand synthesis. The resulting double-stranded cDNA fragments underwent end repair to generate blunt ends, followed by 3′ adenylation to facilitate adapter ligation. Finally, adapter-ligated fragments were purified, size-selected, PCR-amplified, and purified again to generate sequencing-ready cDNA libraries.

2.3. mRNA Sequencing, Quality Assessment, and Read Alignment

A total of 18 samples were sequenced on the Illumina NovaSeq 6000 platform (Illumina, San Diego, CA, USA). Sequencing images were converted to raw FASTQ files by base calling with CASAVA v1.8.2, and samples were distinguished using their index sequences. Library and sequencing quality were evaluated using clean-data yield, sequencing error rate, Q30 score (the percentage of bases with an estimated base-calling accuracy of at least 99.9%),

GC content, duplication rate, and rRNA contamination. After quality control, the clean reads were aligned to the passion fruit reference genome [11] (https://db.cngb.org/data_resources/assembly/CNA0017758/, 25 November 2024) to generate mapped reads for subsequent analyses. The quality of the alignment results was also assessed. Read alignment was performed using STAR (version 2.7.1a; http://code.google.com/p/rna-star/, 25 November 2024). Transcripts were assembled separately for each sample with StringTie (version 2.2.1; https://ccb.jhu.edu/software/stringtie/, 25 November 2024), and the resulting assemblies were merged. Reference-guided transcript assembly was performed using the available reference genome. GffCompare (https://ccb.jhu.edu/software/stringtie/gffcompare.shtml#1, 25 November 2024) was used to compare assembled transcripts with existing annotations and identify novel transcripts. Newly identified transcripts were functionally annotated against the NCBI nonredundant protein (NR), Swiss-Prot, Pfam, EggNOG, Gene Ontology (GO), and Kyoto Encyclopedia of Genes and Genomes (KEGG) databases.

2.4. Gene Expression Quantification and Sample Correlation Analysis

Gene- and transcript-level expression was quantified using RSEM (version 1.3.3). Expression values were reported as transcripts per million (TPM) to account for differences in transcript length and sequencing depth. Gene expression distributions across samples were visualized using box and violin plots. Spearman's rank correlation coefficients were calculated to assess similarities among biological replicates, with values closer to 1 indicating greater concordance. Hierarchical clustering with average linkage and Euclidean distance was visualized using a heatmap. Principal component analysis (PCA) was also used to assess overall expression-profile similarities and identify potential outliers.

2.5. Differentially Expressed Genes

Differential expression analysis was performed on gene/transcript read counts using DESeq2 (version 1.42.0; https://bioconductor.org/packages/release/bioc/html/DESeq2.html, 27 November 2024). Counts were modeled using a negative binomial distribution, and p-values were adjusted for multiple testing using the Benjamini–Hochberg (BH) procedure. Genes with an adjusted p-value < 0.05 and an absolute log2 fold change ($|\log_2 FC|$) ≥ 1 were classified as differentially expressed genes (DEGs).

2.6. GO Enrichment Analysis

GO enrichment analysis was performed using GOATOOLS (version 1.4.4; https://pypi.org/project/goatools/, 27 November 2024). All genes annotated to GO terms were used as the background set. Enrichment was assessed using Fisher's exact test, and p-values were adjusted for multiple testing using the Benjamini–Hochberg (BH) procedure. GO terms with an adjusted p-value < 0.05 were considered significantly enriched.

2.7. KEGG Pathway Enrichment Analysis

KEGG pathway enrichment analysis was performed using R scripts, with all KEGG-annotated genes as the background set. Significance was assessed using a hypergeometric test, which is equivalent to Fisher's exact test in this setting. p-Values were adjusted using the Benjamini–Hochberg (BH) procedure, and pathways with an adjusted p-value < 0.05 were considered significantly enriched. This analysis was used to identify metabolic and signaling pathways associated with the target gene sets.

2.8. Rt-qPCR

Approximately 100 mg of passion fruit tissues were ground in liquid nitrogen, and total RNA was extracted using the CWBIO OminiPlant RNA Kit (DNase I) (CWBIO, Beijing,

China) according to the manufacturer's instructions and stored at −70 °C. RNA concentration and purity were assessed using a NanoDrop 2000; integrity was evaluated by agarose gel electrophoresis, and RQN values were determined using an Agilent 5300 Fragment Analyzer. The RNA template, 5 × HiScript II qRT SuperMix II (Vazyme, Nanjing, China), and RNase-Free Water were thawed and kept on ice. The reaction mixture was prepared as follows: 2 µg RNA template, 4 µL 4 × gDNA Wipper Mix, and RNase-Free Water to a final volume of 16 µL. After gentle pipetting, the mixture was incubated at 42 °C for 15 min to remove gDNA. Subsequently, 4 µL of 5 × HiScript II qRT SuperMix II was added, mixed gently, and the reaction was carried out at 50 °C for 15 min, followed by inactivation at 85 °C for 5 s. After brief centrifugation, the cDNA was cooled on ice. The reverse transcription product was diluted and used as the template for qPCR. The 20 µL PCR mixture contained 10 µL 2 × Universal SYBR qPCR Master Mix (MedChemExpress (MCE), Monmouth Junction, NJ, USA), 0.4 µL each of 10 µM forward and reverse primers, 1 µL cDNA template, and ddH_2O to a final volume of 20 µL. The plate was placed in a Roche LightCycler 480 real-time PCR system (Roche, Basel, Switzerland) and subjected to pre-denaturation at 95 °C, followed by 40 cycles of 95 °C for 15 s, annealing at the temperature specified in the primer information table for 15 s, and 72 °C for 20 s. *EF1* was used as the reference gene [4]. Samples with no Ct value were assigned a value of 35, and the quantitative data were analyzed using the $2^{-\Delta\Delta Ct}$ method [12]. All primers (Supplementary Table S1) were designed using Primer-Premier 5.

2.9. Heat Shock Factor (HSF) Target Gene Analysis

Transcription factor families were predicted from SUPERFAMILY and Pfam annotations generated with InterProScan. SUPERFAMILY and Pfam identifiers, including the HSF-associated Pfam domain PF00447, were obtained for each gene and matched to transcription factor family annotations in the DBD transcription factor prediction database.

Potential HSF target genes were predicted using FIMO. Position weight matrices (PWMs) for transcription factor-binding motifs obtained from JASPAR were used to scan the whole genome or promoter regions, defined as 2 kb upstream to 500 bp downstream of transcription start sites (TSSs). Putative binding sites were identified at $p < 0.0001$. For motifs obtained from PlantTFDB, curated motifs (MP00187, MP00305, MP00371, MP00379, and MP00443) were used directly for sequence matching. Predicted binding sites were assigned to nearby genes to identify potential targets. Where transcriptome expression data were available, correlations between transcription factors and their predicted targets, along with the corresponding *p*-values, were calculated to support the predictions. Relationships showing stronger expression correlations were considered more strongly supported.

2.10. Statistical Analysis

GraphPad Prism 10 software was used to generate plots. Values are presented as the mean ± standard deviation (SD). Pairwise comparisons were performed using two-tailed Student's *t*-tests in Microsoft Excel 2019. Statistical significance is indicated by * $p < 0.05$, ** $p < 0.01$, and *** $p < 0.001$.

3. Results

3.1. Sequencing Data Statistics

Sequencing statistics for all 18 samples are summarized in Table 1. The number of raw reads per sample ranged from 43.53 to 53.59 million, with an average of 48.28 million reads. The total number of raw bases ranged from 6.57 to 8.09 Gb, with a mean of 7.29 Gb. After quality filtering, the number of clean reads ranged from 43.27 to 53.25 million, averaging 47.98 million reads, while the amount of clean data ranged from 6.50 to 7.98 Gb, with an

average of 7.20 Gb. These results indicate a high data retention rate and effective quality-control procedures. Assessment of base-calling quality showed that the sequencing error rate was below 0.012% for all samples, with an average of 0.0117%. The Q20 and Q30 values ranged from 98.91% to 99.03% (mean, 98.96%) and from 96.37% to 96.68% (mean, 96.48%), respectively, indicating high sequencing accuracy and reliable base calling. The GC content ranged from 44.7% to 46.3%, with an average of 45.85%. The limited variation in GC content among samples indicates a relatively uniform base composition with no obvious GC bias. Taken together, these quality metrics demonstrate that the sequencing data were of high quality and met the requirements for subsequent bioinformatic analyses, including differential expression analysis, transcript assembly, and variant detection, thereby providing a reliable basis for downstream data mining and interpretation.

Table 1. Sequencing data information of 18 passion fruit samples.

Sample	Raw Reads	Raw Bases	Clean Reads	Clean Bases	Error Rate (%)	Q20 (%)	Q30 (%)	GC Content (%)
Jinlingziguo1_1	46,047,266	6.953×10^9	45827210	6.875×10^9	0.0117	98.97	96.52	45.26
Jinlingziguo1_2	47,620,408	7.191×10^9	47,379,088	7.107×10^9	0.0117	98.95	96.47	45.79
Jinlingziguo1_3	48,046,888	7.255×10^9	47,750,050	7.171×10^9	0.0117	98.95	96.47	44.7
Jinlingziguo2_1	46,505,370	7.022×10^9	46,199,622	6.936×10^9	0.0117	98.93	96.43	46
Jinlingziguo2_2	48,758,552	7.363×10^9	48,465,238	7.269×10^9	0.0118	98.93	96.38	45.93
Jinlingziguo2_3	48,856,364	7.377×10^9	48,551,732	7.283×10^9	0.0117	98.94	96.43	46
Jinlingziguo3_1	53,588,676	8.092×10^9	53,249,592	7.982×10^9	0.0117	98.98	96.57	45.68
Jinlingziguo3_2	46,332,468	6.996×10^9	46,006,112	6.902×10^9	0.0118	98.91	96.37	45.85
Jinlingziguo3_3	48,635,760	7.344×10^9	48,315,480	7.24×10^9	0.0118	98.93	96.42	45.72
Huangguoyuanshengzhong1_1	51,342,886	7.753×10^9	51,054,882	7.657×10^9	0.0116	99.03	96.68	46.2
Huangguoyuanshengzhong1_2	53,154,668	8.026×10^9	52,787,970	7.928×10^9	0.0118	98.93	96.41	46.09
Huangguoyuanshengzhong1_3	44,593,998	6.734×10^9	44,314,610	6.649×10^9	0.0117	98.96	96.47	46.27
Huangguoyuanshengzhong2_1	46,310,674	6.993×10^9	46,048,544	6.906×10^9	0.0117	98.96	96.47	46.2
Huangguoyuanshengzhong2_2	43,534,532	6.574×10^9	43,271,454	6.496×10^9	0.0117	98.99	96.57	46.19
Huangguoyuanshengzhong2_3	48,901,250	7.384×10^9	48,625,344	7.302×10^9	0.0116	99.01	96.65	46.23
Huangguoyuanshengzhong3_1	48,499,526	7.323×10^9	48,196,452	7.229×10^9	0.0118	98.93	96.39	45.92
Huangguoyuanshengzhong3_2	50,061,176	7.559×10^9	49,735,314	7.463×10^9	0.0117	98.96	96.51	45.95
Huangguoyuanshengzhong3_3	48,197,132	7.278×10^9	47,887,124	7.181×10^9	0.0118	98.93	96.42	45.4

3.2. Alignment to the Reference Genome

Based on alignment of the 18 samples to the passion fruit reference genome (Supplementary Table S2), overall mapping rates ranged from 64.0% to 87.49%, while uniquely mapped read rates ranged from 57.01% to 80.44%. Overall mapping rates for Jinlingziguo samples generally exceeded 80%. In contrast, the Huangguoyuanshengzhong 1 group showed substantially lower mapping rates (64–68%), which may be related to genomic structural variation in this group or incomplete representation of its genomic sequences in the reference genome. Mapping rates for Huangguoyuanshengzhong stages 2 and 3 were comparable to those for Jinlingziguo. The proportions of multimapped reads ranged from 3.78% to 11.5%, potentially reflecting the presence of repetitive genomic regions.

3.3. Analysis and Functional Annotation of Expressed Genes

We detected 32,373 expressed genes, including 29,520 previously annotated and 2853 novel genes. We also identified 56,265 expressed transcripts, comprising 28,357 known and 27,908 novel transcripts. Functional annotation of novel transcripts revealed a substantial proportion associated with retrotransposons. Numerous transcripts were annotated as encoding reverse transcriptase (RVT), integrase (IN), ribonuclease H (RNase H), and zinc-finger domains, and were significantly enriched in Gene Ontology (GO) terms such as DNA integration (GO:0015074) and nucleic acid binding (GO:0003676). Other transcripts were associated with transcriptional regulation, plant defense, hormone signaling,

ubiquitin-mediated protein degradation, cell-wall and carbohydrate metabolism, redox processes, and photosynthesis-related functions.

To identify candidate heat-responsive genes and pathways, we integrated transcript annotations from multiple databases with findings from previous studies of plant abiotic stress. Genes and pathways implicated in heat responses in *Arabidopsis thaliana*, rapeseed, rice, and maize were compiled into a reference database. This database was then used in conjunction with the reference-based transcriptome annotation results to identify candidate heat-responsive genes and pathways in passion fruit. Analysis of abiotic-stress-related KEGG metabolic and signaling pathways among the 32,373 expressed genes identified 19 pathways associated with plant heat stress, including plant hormone signal transduction, plant-pathogen interaction, protein processing in the endoplasmic reticulum, and the MAPK signaling pathway-plant (Figure 1A). Subsequently, we analyzed the associations among the 19 pathways based on shared genes and found that the MAPK signaling pathway-plant and plant hormone signal transduction shared the largest number of genes, with 76 (Figure 1B). In addition, six pathways shared no genes with one another, namely DNA replication, phenylalanine, tyrosine and tryptophan biosynthesis, phenylpropanoid biosynthesis, SNARE interactions in vesicular transport, sulfur relay system, and vitamin B6 metabolism.

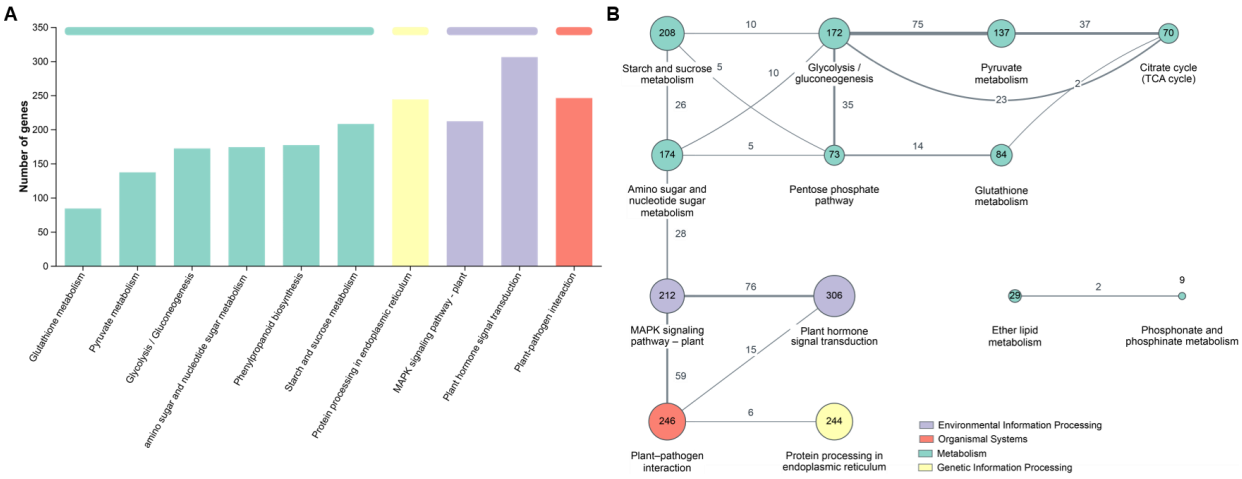

Figure 1. Functional annotation of genes related to high-temperature stress in passion fruit Jinlingziguo and Huangguoyuanshengzhong. (**A**) Pathway enrichment analysis of expressed genes in three developmental stages of passion fruit. (**B**) Correlation analysis among 19 pathways.

3.4. Differential Gene Expression Analysis

Across the three stages of floral development, the mean expression level of the 32,373 detected genes ranged from 24.21 to 24.90 TPM. Principal component analysis (PCA) was performed using the scikit-learn package in Python (v. 3.13). Principal components were calculated using the sklearn decomposition. PCA module, and the variance explained by each component and the coordinates of individual samples in principal-component space were obtained from the covariance structure of the expression data. The three biological replicates within each treatment group clustered closely in the PCA score plot (Figure 2), supporting the reproducibility of the expression measurements.

Differential expression analysis using DESeq2 identified 7529 DEGs across the three stage-specific comparisons. The A1 versus A2 comparison had the most DEGs (4977), followed by C1 versus C2 (3272) and B1 versus B2 (2853). In each comparison, downregulated genes outnumbered upregulated genes. Specifically, A1 vs. A2 contained 2937 downregulated and 2040 upregulated genes, representing the largest transcriptional difference among the three comparisons. In B1 vs. B2, 963 genes were upregulated, and 1890 were

downregulated, whereas C1 vs. C2 contained 818 upregulated and 2454 downregulated genes (Supplementary Figure S1).

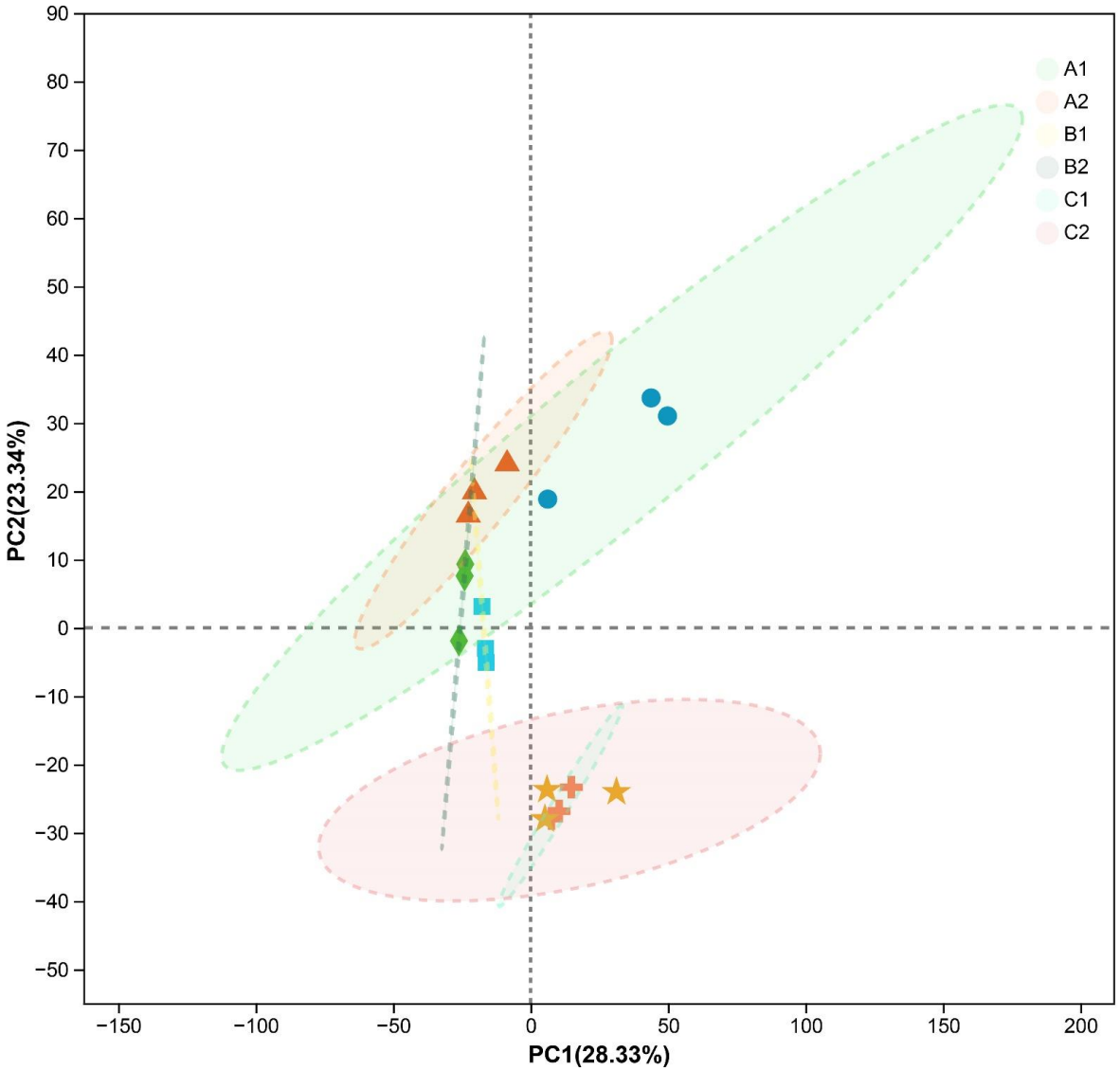

Figure 2. Principal component analysis of expression levels among samples of Jinlingziguo and Huangguoyuanshengzhong.

3.5. Functional Enrichment Analysis of DEGs

To investigate the potential biological functions of the DEGs, Gene Ontology (GO) and KEGG pathway enrichment analyses were performed. GO enrichment analysis using GOATOOLS identified 21 significantly enriched GO terms among 7103 DEGs across the three treatment stages. Of these DEGs, 631 were significantly associated with the "response to stimulus" category and 490 with the "response to stress" category (Figure 3).

KEGG analysis identified 20 significantly enriched pathways among the 7103 DEGs across the three comparisons. Based on a reference database of heat-stress-associated genes and pathways from *Arabidopsis thaliana*, rapeseed, rice, and maize, 107 DEGs were assigned to plant hormone signal transduction, 25 to DNA replication, 79 to starch and sucrose metabolism, and 76 to the plant MAPK signaling pathway (Figure 4).

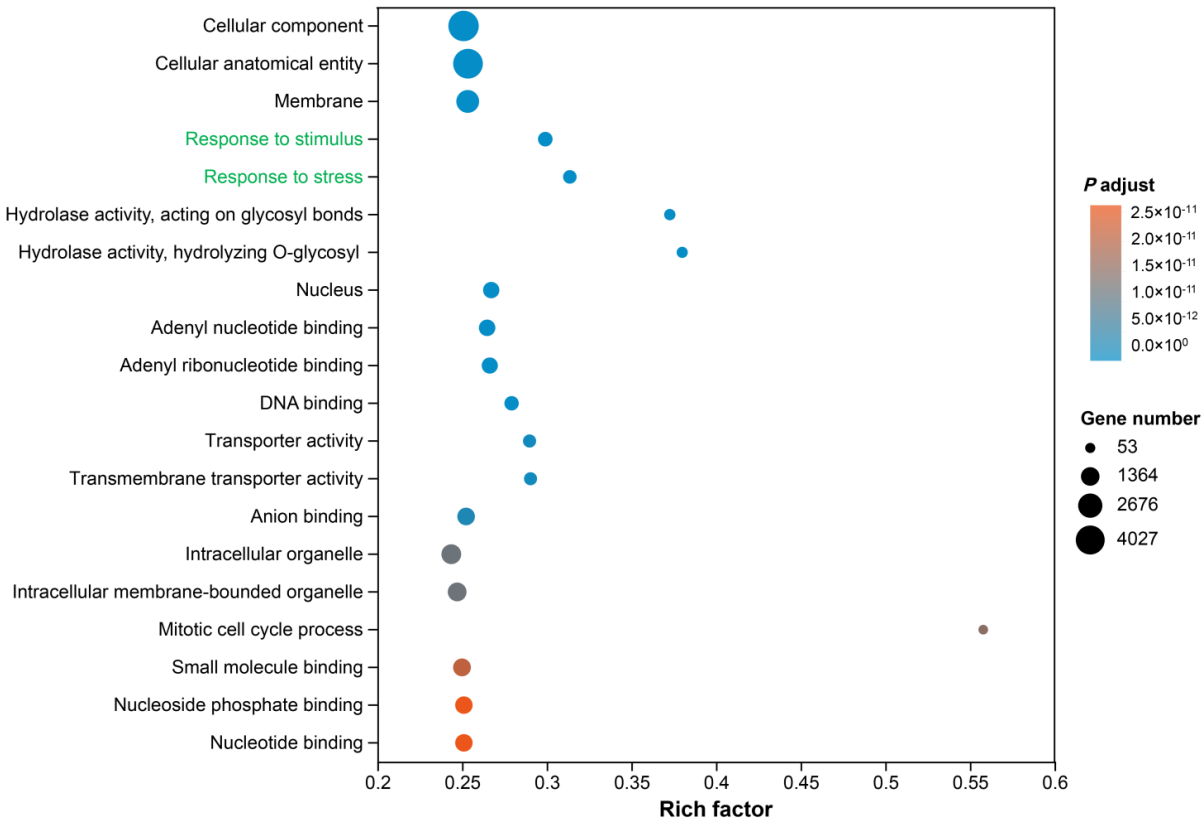

Figure 3. GO functional enrichment analysis of DEGs at three developmental stages of flowers in Jinlingziguo and Huangguoyuanshengzhong.

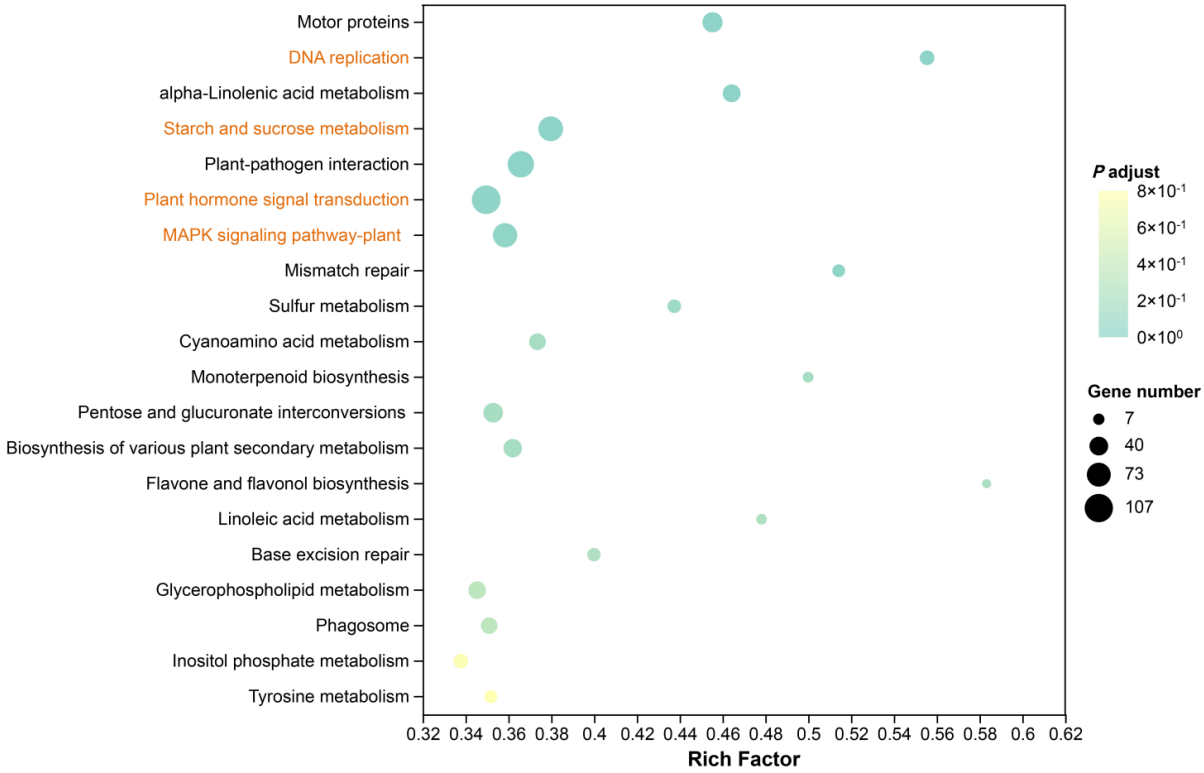

Figure 4. KEGG pathway enrichment analysis of DEGs at three developmental stages of flowers in Jinlingziguo and Huangguoyuanshengzhong.

3.6. WGCNA and Molecular Regulatory Network Analysis

Gene expression data were normalized using DESeq2, and genes with atypical expression patterns or low variation were filtered before weighted gene co-expression network analysis (WGCNA). Network parameters were selected to approximate a scale-free topology. After filtering, 14,937 genes remained for analysis. The scale-free topology fit curve is presented in Supplementary Figure S2 ($R^2 = 0.5096$). A soft-thresholding power of 9 was used to construct the network, giving greater weight to stronger gene–gene correlations.

Following data preprocessing, genes with similar expression patterns were grouped into co-expression modules. A total of 18 modules were identified, each containing 40–4497 genes (Supplementary Figure S3). Module–trait association analysis highlighted three modules: green-yellow and pink. KEGG analysis associated the green-yellow module with basal transcription factors (*ZX.01G0050650*) and plant hormone signal transduction (*ZX.01G0041600*, *ZX.01G0032990*, *ZX.01G0041270*, *ZX.02G0020960*, and *ZX.08G0012950*) (Figure 5). The pink module was associated with the MAPK signaling pathway (*ZX.01G0041270* and *ZX.01G0053160*) and plant hormone signal transduction (*ZX.01G0041270*) (Figure 6). Weighted gene co-expression networks were subsequently constructed for the green-yellow module (Supplementary Figure S4) and the pink module (Supplementary Figure S5). *ZX.04G0014930* and *ZX.01G0041270* were identified as hub genes in the pink and green-yellow modules, respectively. An integrated network of the two modules was also constructed (Figure 7). These candidate genes provide potential targets for further investigation of heat tolerance in passion fruit.

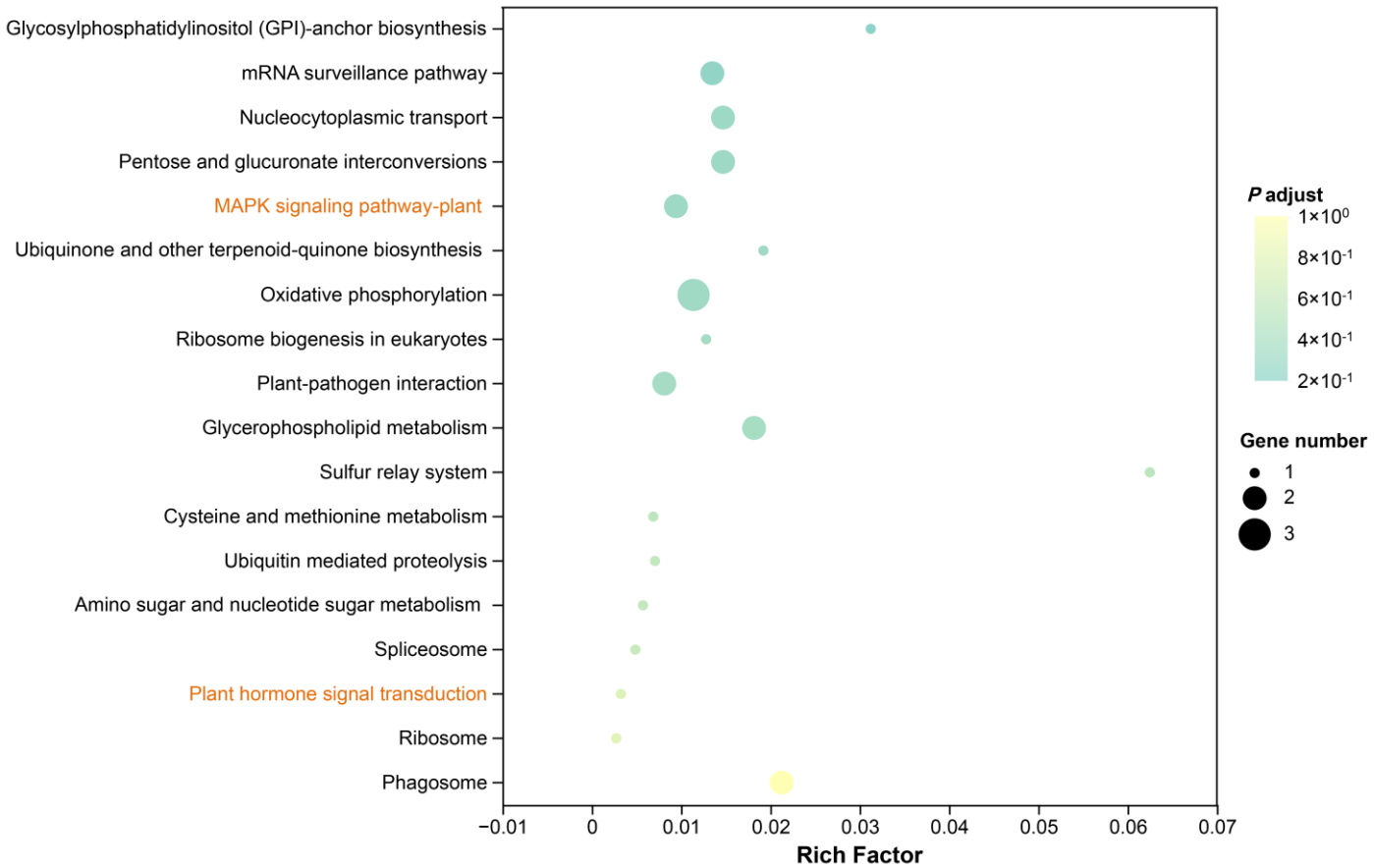

Figure 5. KEGG pathway enrichment analysis of 319 genes in the green-yellow module.

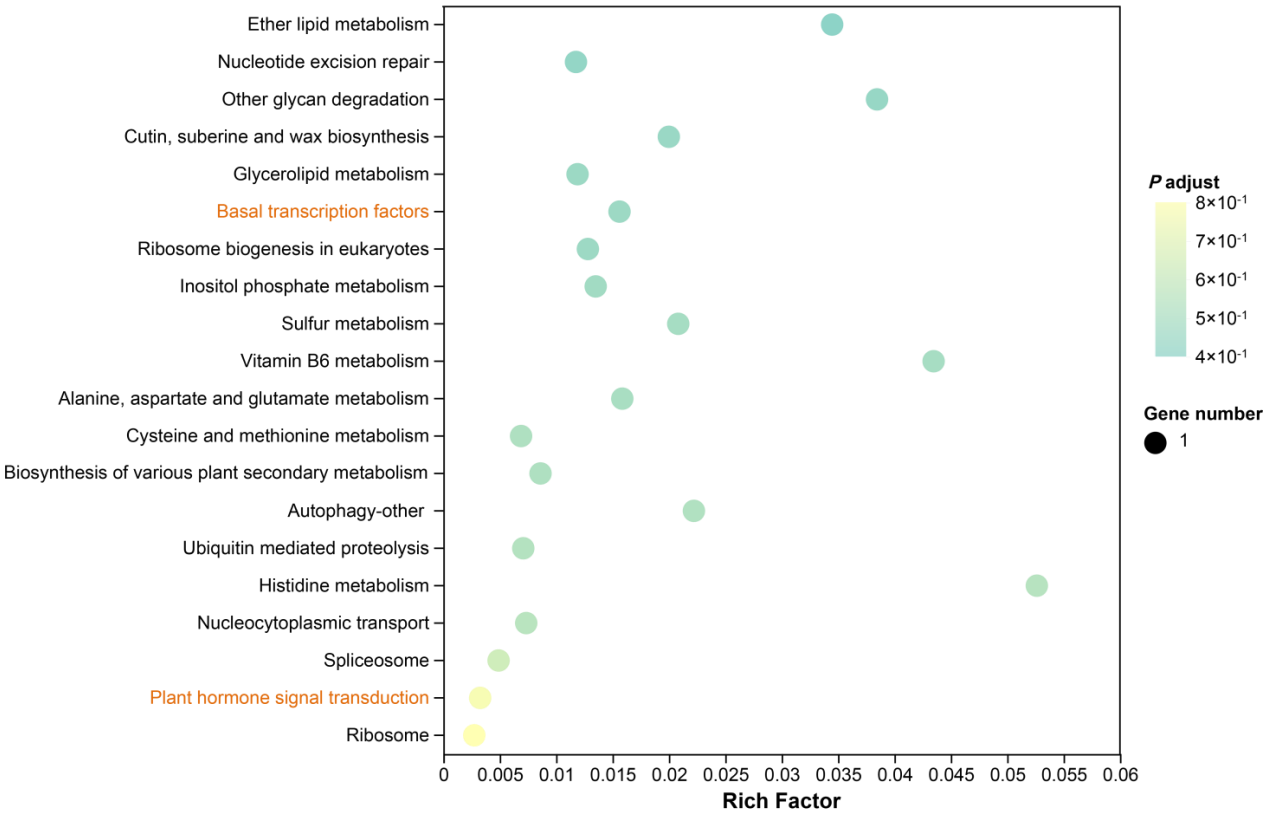

Figure 6. KEGG pathway enrichment analysis of 439 genes in the pink module.

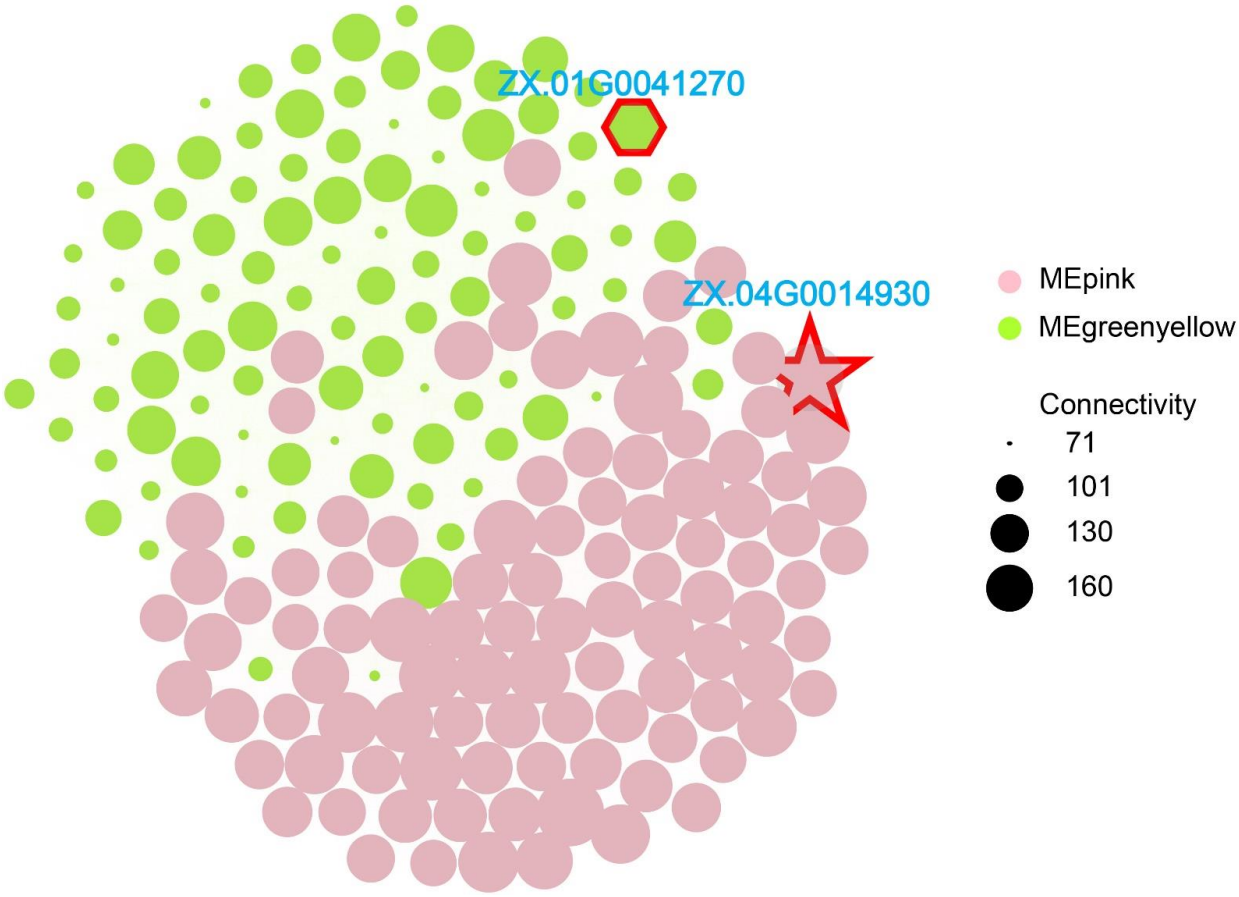

Figure 7. Hub genes and regulatory network of the pink and green-yellow modules.

3.7. Functional Prediction of HSF Target Genes

Transcription factor prediction identified 28 HSF genes in passion fruit, corresponding to 43 transcripts. The gene-to-transcript ratio of approximately 1:1.54 is consistent with the possibility of alternative splicing within this family. We predicted 2537 potential target genes for the 28 HSFs. GO enrichment analysis associated eight targets (*ZX.01G0009280*; *ZX.01G0011610*; *ZX.01G0011790*; *ZX.01G0021880*; *ZX.01G0048300*; *ZX.01G0076260*; *ZX.02G0018740*; *ZX.05G0011540*) with 'response to temperature stimulus'. Thirteen targets (*ZX.01G0009280*; *ZX.01G0011610*; *ZX.01G0011790*; *ZX.01G0021880*; *ZX.01G0033890*; *ZX.01G0048300*; *ZX.01G0076260*; *ZX.01G0126190*; *ZX.02G0018740*; *ZX.05G0011540*; *ZX.08G0009630*; *ZX.08G0028950*; *ZX.09G0018330*) were associated with 'response to abiotic stimulus'. KEGG analysis linked three targets (*ZX.09G0010120*, *ZX.03G0016190*, and *ZX.01G0020170*) to the plant MAPK signaling pathway and four (*ZX.03G0006300*, *ZX.09G0010120*, *ZX.08G0014210*, and *ZX.03G0016190*) to plant hormone signal transduction.

3.8. Identification of Hub Candidate Genes

Based on the expression levels in the Supplementary Table S3, *ZX.01G0032990* was generally higher in Jinlingziguo than in Huangguoyuanshengzhong, and relatively high in Jinlingziguo3; *ZX.01G0041270* was barely expressed in Huangguoyuanshengzhong but clearly expressed in Jinlingziguo; *ZX.01G0041600* was relatively high in Huangguoyuanshengzhong at the early stage and decreased at the late stage, and was also relatively low in Jinlingziguo at the late stage; *ZX.01G0050650* was relatively high in Huangguoyuanshengzhong1 and similar to Jinlingziguo at the other stages; *ZX.01G0053160* showed low expression in Huangguoyuanshengzhong and extremely high expression in Jinlingziguo; both *ZX.02G0020960* and *ZX.08G0012950* showed higher expression in Jinlingziguo than in Huangguoyuanshengzhong, with the latter being relatively high in Jinlingziguo3; *ZX.04G0014930* was generally higher in Huangguoyuanshengzhong than in Jinlingziguo, and both varieties showed a decrease with stage; *ZX.04G0030270* was expressed at a low level only in Huangguoyuanshengzhong and was not detected in any Jinlingziguo samples; *ZX.05G0014510* was very high in individual replicates of Huangguoyuanshengzhong1 and lower in the others, and was overall very low in Jinlingziguo. To assess the reliability of the RNA-seq results, we measured the expression of 10 selected genes at three floral developmental stages by RT-qPCR. The results showed that the RT-qPCR results for all 10 genes were consistent with the RNA-Seq results (Figure 8). Among them, expression patterns of *ZX.01G0032990*, *ZX.01G0041270*, *ZX.01G0050650*, *ZX.04G0014930*, and *ZX.08G0012950* were highly consistent with the RNA-Seq results, indicating that the transcriptome sequencing data had good accuracy. Among them, *ZX.01G0041270*, a core gene for heat tolerance in passion fruit, is a homolog of *Arabidopsis AT5G57050* (*ABI2*). Studies have shown that *abi2*, as an Abscisic acid (ABA) signaling pathway mutant, has the strongest defect in acquired thermotolerance in *Arabidopsis* [13]. *ZX.01G0041270* is highly homologous to *LOC_Os01g40094* (*OsABIL1*) and *LOC_Os05g51510* (*OsABIL2*), and both *OsABIL1* and *OsABIL2* negatively regulate the ABA signaling pathway [14,15]. In summary, we consider *ZX.01G0041270* an ideal candidate gene.

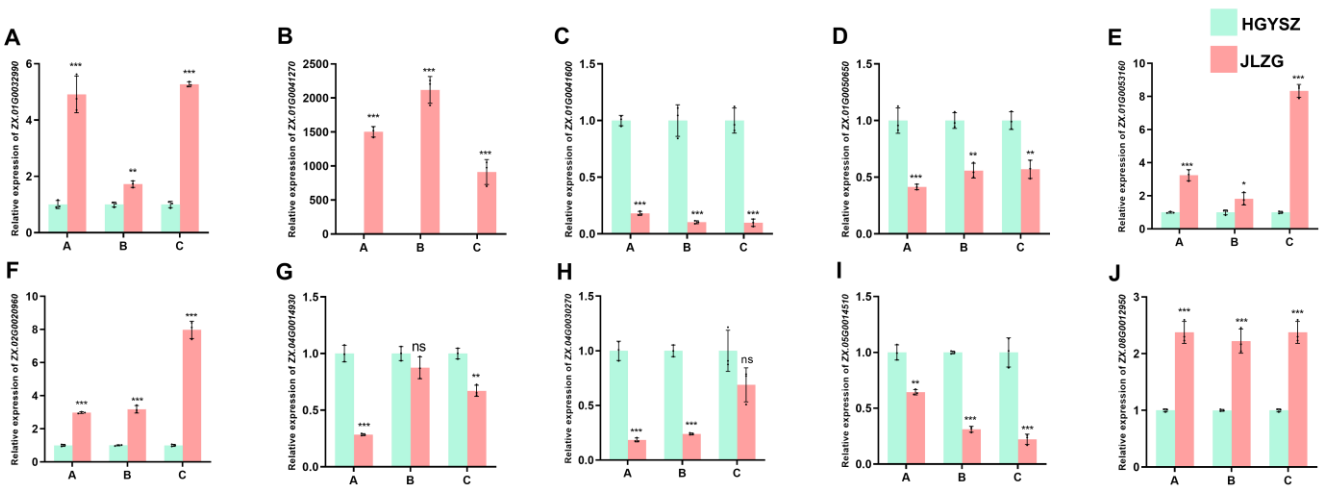

Figure 8. Relative expression of 10 candidate genes in JLZG and HGYSZ were detected using RT-qPCR. (**A**–**J**): *ZX.01G0032990*, *ZX.01G0041270*, *ZX.01G0041600*, *ZX.01G0050650*, *ZX.01G0053160*, *ZX.02G0020960*, *ZX.04G0014930*, *ZX.04G0030270*, *ZX.05G0014510*, and *ZX.08G0012950*. Data are shown as means ± SD (n = 3). * $p < 0.05$, ** $p < 0.01$, *** $p < 0.001$ (two-tailed Student's *t* test), ns: not significant. JLZG: Jinlingziguo, HGYSZ: Huangguoyuanshengzhong.

4. Discussion

High-temperature stress disrupts floral organ formation and development in passion fruit, ultimately reducing yield. In the present study, a total of 7529 differentially expressed genes (DEGs) were identified across three floral developmental stages. At each stage, the number of downregulated genes exceeded the number of upregulated genes, with the most pronounced difference observed in the A1 vs. A2 comparison, which contained 2937 downregulated and 2040 upregulated genes. This pattern is consistent with previous transcriptomic studies of heat stress in passion fruit, which reported a general suppression of gene expression under elevated temperatures [4]. Notably, although Jinlingziguo exhibited a greater number of downregulated genes at all developmental stages (Supplementary Figure S1), Jinlingziguo was still able to maintain a relatively stable flowering process under high-temperature conditions. This observation suggests that heat tolerance in Jinlingziguo may not depend primarily on the broad activation of stress-responsive genes, but rather on maintaining stable expression of genes essential for floral development. The early developmental stage (stage A) showed the greatest number of DEGs, suggesting heightened sensitivity to heat at this stage. Early bud development includes processes such as floral primordium initiation and specification of floral organ identity; disruption of these processes could affect subsequent flower development. This finding is consistent with the study by Sobol et al. [2], which demonstrated an important role for cytokinins in protecting floral primordia and further suggests that disruption of early floral development by high temperature may represent a major molecular basis for heat-induced yield loss.

Weighted gene co-expression network analysis identified the pink and green-yellow modules as key modules associated with heat-tolerance-related traits. The pink module was enriched in MAPK signaling and plant hormone signal transduction, whereas the green-yellow module was enriched in basal transcription factors and plant hormone signal transduction. *ZX.04G0014930* and *ZX.01G0041270* were identified as hub genes in the pink and green-yellow modules, respectively. The association of *ZX.01G0041270* with both MAPK and hormone signaling suggests that it may participate in coordination between these pathways.

The MAPK cascade is a central hub in plant stress signal transduction and plays a critical intermediary role in responses to heat stress [16]. The enrichment of MAPK-related DEGs

and co-expression module genes in our study suggests that MAPK signaling is involved in the heat response of passion fruit floral organs. At the same time, the coordinated enrichment of plant hormone signal transduction pathways further supports a model of MAPK-hormone signaling integration, in which heat-stress signals are transmitted through MAPK cascades to hormone signaling pathways, thereby modulating the metabolism and responses of hormones such as auxin, gibberellin, cytokinin, and abscisic acid [17] and ultimately influencing floral organ developmental fate. Both hub genes identified in the key modules were linked to hormone signaling, while *ZX.01G0041270* was associated with both MAPK and hormone pathways. These observations identify potential points of pathway convergence, although their regulatory relationships remain to be established experimentally.

Heat shock factors (HSFs) are major regulatory hubs in heat-stress signaling, and their central roles in plant thermotolerance have been demonstrated in multiple crop species [18,19]. Here, we identified 28 HSF family members in passion fruit and predicted 2537 potential target genes. GO analysis associated eight targets with responses to temperature stimuli and 13 with responses to abiotic stimuli. KEGG analysis further linked three targets to the MAPK signaling pathway and four to plant hormone signal transduction.

The approximately 1:1.54 ratio of HSF genes to transcripts suggests that alternative splicing may contribute to HSF transcript diversity. This observation is consistent with the findings of Wang et al. [5] in their analysis of the passion fruit HSF family and suggests that alternative splicing may represent an additional layer of regulation contributing to HSF-mediated heat tolerance. Enrichment of the 'response to temperature stimulus' and 'response to abiotic stimulus' categories among predicted HSF targets suggests that HSFs could regulate a broader set of stress-responsive genes beyond classical heat shock proteins. Their predicted targets also included genes associated with MAPK and plant hormone signaling, consistent with potential interactions among these pathways. However, the predicted regulatory relationships will require experimental validation before HSFs can be assigned specific positions within this network.

ABA plays an important role in regulating heat stress tolerance in plants. In this study, the passion fruit heat tolerance-related candidate gene *ZX.01G0041270* is a homolog of *Arabidopsis ABI2*. *ABI2* encodes a protein phosphatase 2C that participates in ABA signal transduction and functions as a negative regulator of ABA signaling [13]. *ZX.01G0041270* is also highly homologous to *LOC_Os01g40094* (*OsABIL1*) and *LOC_Os05g51510* (*OsABIL2*), and both *OsABIL1* and *OsABIL2* negatively regulate the ABA signaling pathway [14,15]. As one of the stress signal integration nodes in the plant response to high-temperature tolerance, ABA coordinates stomatal and ROS signaling responses, induces the HSF–HSP core transcriptional–protein quality control module [20,21], and exhibits antagonistic and synergistic interactions with hormones such as BR, thereby integrating high-temperature, drought, and endogenous developmental signals and helping balance water retention and heat dissipation, ROS signaling and scavenging, and heat-stress defense and growth [22]. Based on its sequence homology and the established functions of related phosphatases, *ZX.01G0041270* may negatively regulate ABA signaling and contribute to adaptation to elevated temperatures in passion fruit. Direct functional studies are needed to test this hypothesis.

5. Conclusions

In this study, transcriptome sequencing was performed using two passion fruit germplasms with markedly different levels of heat tolerance, Jinlingziguo and Huangguoyuanshengzhong, to characterize the molecular responses associated with floral organ formation under high-temperature stress. Differential expression analysis highlighted the early stage of floral development as particularly responsive to elevated temperature.

WGCNA identified two key co-expression modules associated with MAPK signaling and plant hormone signal transduction, with *ZX.04G0014930* and *ZX.01G0041270* as candidate hub genes. *ZX.01G0041270* may affect the heat tolerance of passion fruit by regulating the ABA signaling pathway. Analysis of predicted HSF targets further suggested potential connections among HSF activity, MAPK signaling, and hormone responses. These results provide candidate genes and a framework for future functional studies and the breeding of heat-tolerant passion fruit cultivars.

Supplementary Materials: The following supporting information can be downloaded at: https://www.mdpi.com/article/10.3390/cimb48111265/s1.

Author Contributions: Conceptualization, Y.W. and H.M.; data curation, W.H.; funding acquisition, Y.W.; investigation, J.L. and J.Z.; methodology, Y.W. and J.L.; validation, Q.T. and J.L.; writing—original draft; writing—review and editing, X.Y. and H.M. All authors have read and agreed to the published version of the manuscript.

Funding: This work was supported by the National Natural Science Foundation of China (No. 32260740 and 32060660), the Guangxi Natural Science Foundation of China (2023GXNSFAA026301), and the Guangxi Academy of Agricultural Sciences (Guinongke 2026YT118 and Gui TS2022010).

Institutional Review Board Statement: Not applicable.

Informed Consent Statement: Not applicable.

Data Availability Statement: The RNA-seq raw data reported in this paper are available in the NCBI Sequence Read Archive (https://submit.ncbi.nlm.nih.gov/subs/sra/, 29 October 2026) under accession number PRJNA1553524 (from SRR41476402 to SRR41476419).

Conflicts of Interest: The authors declare no conflicts of interest.

Abbreviations

The following abbreviations are used in this manuscript:

ABA	abscisic acid
BR	brassinosteroid
DEGs	differentially expressed genes
FIMO	Find Individual Motif Occurrences
GO	Gene Ontology
HSP	heat shock protein
HSF	heat shock factor
KEGG	Kyoto Encyclopedia of Genes and Genomes
MAPK	mitogen-activated protein kinase
PCA	principal component analysis
PCR	polymerase chain reaction
PWM	position weight matrix
RNA-Seq	RNA sequencing
ROS	reactive oxygen species
RQN	RNA quality number
RT-qPCR	reverse transcription quantitative polymerase chain reaction
TPM	transcripts per million
TSS	transcription start site
WGCNA	weighted gene co-expression network analysis

References

1. Zheng, Y.Y.; Chen, L.H.; Fan, B.L.; Xu, Z.; Wang, Q.; Zhao, B.Y.; Gao, M.; Yuan, M.H.; Tahir, U.M.; Jiang, Y.; et al. Integrative multiomics profiling of Passion fruit reveals the genetic basis for fruit color and aroma. *Plant Physiol.* **2024**, *194*, 2491–2510. [CrossRef] [PubMed]
2. Sobol, S.; Chayut, N.; Nave, N.; Kafle, D.; Hegele, M.; Kaminetsky, R.; Wünsche, J.N.; Samach, A. Genetic variation in yield under hot ambient temperatures spotlights a role for cytokinin in protection of developing floral primordia. *Plant Cell Environ.* **2014**, *37*, 643–657. [CrossRef] [PubMed]

3. De Almeida, O.L.; Nguyen, N.; Kenth, S.D.; Dabirimirhosseinlo, M.; Terada, N.; Sanada, A.; Koshio, K. Responses under heat and cold stress in Passiflora edulis f. flavicarpa. *Int. J. Mol. Sci.* **2026**, *27*, 3811. [CrossRef] [PubMed]
4. Wang, H.; Zhao, J.; Lai, M.; Zhang, Y.; Qiu, W.; Li, Y.; Tu, H.; Ling, Q.; Fu, X. Differential gene expression analysis and physiological response characteristics of Passion fruit (*Passiflora edulis*). *PeerJ* **2023**, *11*, e14839. [CrossRef] [PubMed]
5. Wang, L.; Liu, Y.; Chai, G.; Zhang, D.; Fang, Y.; Deng, K.; Aslam, M.; Niu, X.; Zhang, W.; Qin, Y.; et al. Identification of Passion fruit HSF gene family and the functional analysis of PeHSF-C1a in response to heat and osmotic stress. *Plant Physiol. Biochem.* **2023**, *200*, 107800. [CrossRef] [PubMed]
6. Xing, W.; Wu, B.; Zhang, J.; Yang, S.; Zhou, W.; Ma, F.; Huang, D.; Hu, W.; Li, H.; Meng, C.; et al. Investigation of the HSF transcription factor, expression characteristics and stress tolerance function of PeHSF-2 in Passion fruit (*Passiflora edulis*). *Plant Physiol. Biochem.* **2026**, *233*, 111169. [CrossRef] [PubMed]
7. Chen, G.; Xu, Y.; Gui, J.; Huang, Y.; Ma, F.; Wu, W.; Han, T.; Qiu, W.; Yang, L.; Song, S. Transcription factors and the heat-tolerant function of PeDof-11 in Passion fruit (*Passiflora edulis*). *Int. J. Mol. Sci.* **2023**, *24*, 12091. [CrossRef] [PubMed]
8. Shad, M.A.; Wu, S.; Wu, Y.; Zhang, L.; Zhou, Y.; Wang, J.; Wang, L.; Ma, C.; Hu, L. Evolution and functional dynamics of the bag gene family in Passion fruit (*Passiflora edulis*). *Plants* **2025**, *14*, 2887. [CrossRef] [PubMed]
9. Jiang, X.; Miao, J.; Zu, W.; Zhou, R.; Zheng, L.; Wei, Y.; Lai, C.; Qin, R.; Zheng, P.; Wei, X.; et al. Functional characterization of KNOX and BELL genes in temperature-responsive floral morphogenesis of Passion fruit (*Passiflora edulis*). *Plants* **2025**, *14*, 1440. [CrossRef] [PubMed]
10. Ma, F.; Zhou, H.; Xu, Y.; Huang, D.; Wu, B.; Xing, W.; Chen, D.; Xu, B.; Song, S. Comprehensive analysis of bZIP transcription factors in Passion fruit. *iScience* **2023**, *26*, 106556. [CrossRef] [PubMed]
11. Ma, D.; Dong, S.; Zhang, S.; Wei, X.; Xie, Q.; Ding, Q.; Xia, R.; Zhang, X. Chromosome-level reference genome assembly provides insights into aroma biosynthesis in Passion fruit (*Passiflora edulis*). *Mol. Ecol. Resour.* **2021**, *21*, 955–968. [CrossRef] [PubMed]
12. Livak, K.J.; Schmittgen, T.D. Analysis of relative gene expression data using real-time quantitative PCR and the 2(-Delta Delta C(T)) Method. *Methods* **2001**, *25*, 402–408. [PubMed]
13. Larkindale, J.; Hall, J.D.; Knight, M.R.; Vierling, E. Heat stress phenotypes of Arabidopsis mutants implicate multiple signaling pathways in the acquisition of thermotolerance. *Plant Physiol.* **2005**, *138*, 882–897. [CrossRef] [PubMed]
14. Zou, X.; Zhu, Y.; Ma, M.; Li, M.; Wang, X.; Zeng, H.; Yin, C.; Lin, Y. OsPP2C06 positively regulates rice yield by enhancing photosynthesis via negative regulation of abscisic acid signaling. *Int. J. Biol. Macromol.* **2026**, *346*, 150653. [CrossRef] [PubMed]
15. Li, C.; Shen, H.; Wang, T.; Wang, X. ABA regulates subcellular redistribution of OsABI-LIKE2, a negative regulator in ABA signaling, to control root architecture and drought resistance in Oryza sativa. *Plant Cell Physiol.* **2015**, *56*, 2396–2408. [CrossRef] [PubMed]
16. Mo, S.; Qian, Y.; Zhang, W.; Qian, L.; Wang, Y.; Cailin, G.; Ding, H. Mitogen-activated protein kinase action in plant response to high-temperature stress: A mini review. *Protoplasma* **2021**, *258*, 477–482. [CrossRef] [PubMed]
17. Liu, S.; Xing, M.; Yin, X. MAPK regulates secondary metabolism and abiotic stress in horticultural and medicinal plants. *Hortic. Res.* **2025**, *13*, uhaf350. [CrossRef] [PubMed]
18. Feng, Y.; Xia, P. Heat shock transcription factors as integrative hubs for plant stress adaptation: Decoding regulatory networks toward climate-resilient crop design. *Plant Cell Environ.* **2025**, *48*, 8985–9001. [CrossRef] [PubMed]
19. Andrási, N.; Pettkó-szandtner, A.; Szabados, L. Diversity of plant heat shock factors: Regulation, interactions, and functions. *J. Exp. Bot.* **2021**, *72*, 1558–1575. [CrossRef] [PubMed]
20. Kan, Y.; Mu, X.R.; Gao, J.; Lin, H.X.; Lin, Y. The molecular basis of heat stress responses in plants. *Mol. Plant* **2023**, *16*, 1612–1634. [CrossRef] [PubMed]
21. Crawford, T.; Pratx, L.; Bäurle, I. Principles and mechanisms of plant acclimation to heat stress. *Nat. Rev. Mol. Cell Biol.* **2026**, *27*, 668–683. [CrossRef] [PubMed]
22. Chen, Z.; Galli, M.; Gallavotti, A. Mechanisms of temperature-regulated growth and thermotolerance in crop species. *Curr. Opin. Plant Biol.* **2022**, *65*, 102134. [CrossRef] [PubMed]

Disclaimer/Publisher's Note: The statements, opinions and data contained in all publications are solely those of the individual author(s) and contributor(s) and not of MDPI and/or the editor(s). MDPI and/or the editor(s) disclaim responsibility for any injury to people or property resulting from any ideas, methods, instructions or products referred to in the content.